



# Extremely dark GRBs: the case of GRB 100614A and GRB 100615A

V. D'Elia<sup>1,2</sup> and G. Stratta<sup>1,2</sup>

<sup>1</sup> ASI-Science Data Center, Via Galileo Galilei, I-00044 Frascati, Italy

<sup>2</sup> INAF-Osservatorio Astronomico di Roma, Via Frascati 33, I-00040 Monteporzio Catone, Italy e-mail: delia@asdc.asi.it

## Abstract.

Dark gamma-ray bursts (GRBs) are sources with a low optical-to-X-ray flux ratio. Proposed explanations for this darkness are: i) the GRB is at high redshift ii) dust in the GRB host galaxy absorbs the optical/NIR flux iii) GRBs have an intrinsically faint afterglow emission. Within this framework, GRB 100614A and GRB 100615A are extreme. In fact, they are bright in the X-rays, but no optical/NIR afterglow has been detected for either source, despite several follow-up campaigns began early after the triggers. We analyze the X-ray data and collect all the optical/NIR upper limits in literature for these bursts. We then build optical-to-X-ray spectral energy distributions (SEDs) at the times at which the reddest upper limits are available, and we model our SEDs with the extinction curves of the Milky Way (MW), Small Magellanic Cloud (SMC), and the attenuation curve obtained for a sample of starburst galaxies. We find that to explain the deepest NIR upper limits assuming either a MW or SMC extinction law, a visual extinction of  $A_V > 50$  is required, which is extremely unlikely. Since both GRBs are bright in X-rays, explanation iii) also cannot explain their dark classification, unless optical radiation and X-rays are not part of the same synchrotron spectrum. An alternative, or complementary explanation of the previous possibility, involves greyer extinction laws. A starburst attenuation curve gives  $A_V > 10$ , which is less extreme, despite still very high. Assuming high redshift in addition to extinction, implies an  $A_V > 10$  at  $z = 2$  and  $A_V > 4 - 5$  at  $z = 5$ , regardless of the adopted extinction recipe. A different, exotic possibility would be an extremely high redshift origin ( $z > 17$  given the missing K detections). Population III stars are expected to emerge at  $z \sim 20$  and can produce GRBs with energies well above those inferred for our GRBs at these redshifts. Mid- and far-IR observations of these extreme class of GRBs can help us to differentiate between the proposed scenarios.

**Key words.** gamma rays: bursts - cosmology: observations

## 1. Introduction

Long-duration gamma-ray bursts (GRBs) are high energy phenomena linked to the death of massive stars, emitting most of their radiation

*Send offprint requests to:* V. D'Elia

in the hundreds of keV range. The gamma-ray (or prompt) event is followed by an afterglow at longer wavelengths, which has proven crucial to understand the physics of these sources and to investigate the nature of their surrounding medium.

While the X-ray (0.1-10 keV) afterglows are detected in virtually all GRBs, the optical/near infrared (NIR) counterparts are more elusive. Just a few months after the discovery of the first optical counterpart of a GRB (van Paradijs et al. 1997), the search for an optical afterglow associated to GRB 970828 was unsuccessful (Groot et al. 1998) leading to the definition of ‘dark burst’ for a GRB with an X-ray counterpart, but not an optical one. Initially, this lack of detection was widely ascribed to the delay time between the GRB event and optical observations, since ground-based facilities could be on target only hours after the trigger, when the afterglow had faded below their sensitivity limit.

The main scientific driver of the *Swift* satellite was to facilitate the GRB afterglow detection by quickly repointing its narrow field instruments and disseminating the GRB coordinates worldwide. The quick detection with XRT and the increasing number of ground-based automated facilities dramatically improved the optical follow-up success, reducing the fraction of dark GRBs. The definition of dark GRB was reconsidered in a more quantitative manner, based on the expected spectral behaviour in the context of the most commonly accepted scenario of the fireball model. Van der Horst et al. (2009) propose to classify a dark GRB using only the spectral indices of the power-law slopes in the optical ( $\beta_O$ ) and X-ray ( $\beta_X$ ) data, where  $\beta$  is linked to the flux by the relation  $F_\nu \propto \nu^{-\beta}$ . They noted that, regardless of many assumptions on the specific electron energy distribution, if both the optical and X-ray radiation are produced by synchrotron emission from the same source,  $\beta_O$  and  $\beta_X$  are linked. In particular,  $\beta_O = \beta_X - 0.5$  if the cooling frequency lies between the optical and the X-rays, and  $\beta_O = \beta_X$  otherwise. Thus, the optical-to-X-ray spectral index allowed range is  $\beta_X - 0.5 \leq \beta_{OX} \leq \beta_X$ , with  $\beta_{OX} = \beta_X - 0.5$  if a spectral break is present just below the lowest X-ray energy detected. GRB afterglows with  $\beta_{OX} < \beta_X - 0.5$  are classified as dark in this picture.

The optical darkness can be ascribed to different factors (see e.g., Perley et al. 2009): i) the GRB can be at high redshift, so that the

Lyman- $\alpha$  absorption prevents optical identifications; ii) dust in the GRB host galaxy or along the line of sight can absorb the optical afterglow counterpart; iii) the optical faintness can have an intrinsic origin. In this case, however, also the X-ray counterpart is expected to be faint.

Here we study the ‘darkness’ properties of two GRBs (namely, GRB 100614A and GRB 100615A), which are very bright in X-rays, but are not detected in the optical/near-IR band and have no reported host galaxy candidate. The next section summarizes the observations of these two sources and our analysis method. Sect. 3 illustrates our results, and in Sect. 4 we discuss our findings and draw our conclusions. Decay, photon, and spectral indices are indicated with  $\alpha$ ,  $\Gamma$ , and  $\beta$ , following the standard convention  $t^{-\alpha}$ ,  $N_{ph}^{-\Gamma}$ , and  $\nu^{-\beta}$ , respectively.

## 2. Observations and analysis

GRB 100614A and 15A were both discovered by *Swift*-BAT and immediately repointed by XRT and UVOT. XRT reported an extremely bright transient in both cases, while UVOT did not detect any optical counterpart. The two sources were followed-up by several ground-based facilities, beginning 4 hr and 24 minutes after the trigger, respectively, but no optical/NIR counterpart down to the K band has been detected. GRB 100615A has been observed even 9.2 days after the trigger in a deep, K band exposure, but again no counterpart has been found. All the data collected for these two bursts are plotted in Fig. 1. We refer the reader to D’Elia & Stratta (2011) for a full description of the observations of these GRBs and for a comprehensive reference list.

### 2.1. Analysis

We extract the optical to X-ray spectral energy distribution (SED) for both GRBs by selecting those epochs at which we have the deepest and reddest observations (i.e. less affected by any dust extinction), to constrain at best the intrinsic optical afterglow flux upper limit. In addition, we attempt to select an epoch not too

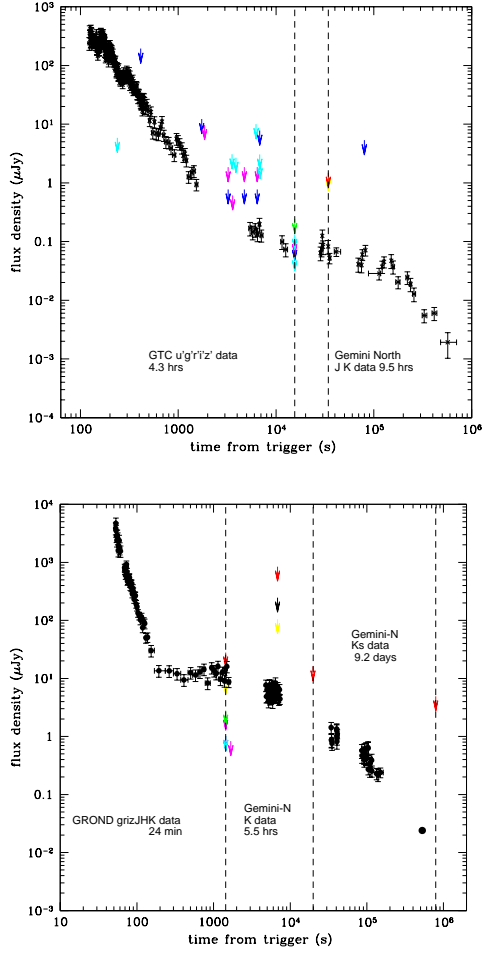


**Fig. 1.** The GRB 100614A (upper panel) and GRB 100615A (bottom panel) X-ray lightcurves, together with all the optical/NIR upper limits estimated using several ground-based facilities (see D’Elia & Stratta 2011 for details). Cyan, blue, magenta, green, yellow, black and red upper limits represents the  $g'$  (and all those bands bluer than  $g'$ ), R, I, z, J, H, K bands, respectively. Vertical dashed lines emphasize the reddest observations and the time at which they have been obtained. Such observations are used in our analysis. The faintest X-ray data in the bottom panel draws the GRB 100615A *Chandra* observation.

close to the initial X-ray steep decay, which is thought to be produced by a different com-

ponent than the one responsible for the afterglow emission. Magnitudes reported in literature were corrected for Galactic absorption ( $E(B-V) = 0.03$  and  $0.047$  for GRB 100614A and 15A, respectively).

A broken power-law model was fitted to the XRT data following the van der Horst et al. (2009) method, therefore fixing the SED normalization and the high-energy spectral index to the value obtained from our X-ray data analysis (within its 90% confidence range), the spectral break at the X-ray energies and the optical to X-ray spectral index as  $\beta_{OX} = \beta_X - 0.5$ .

We model the optical suppression from the X-ray extrapolation assuming either a Milky Way (MW) or a Small Magellanic Cloud (SMC) extinction curve. We also test the attenuation curve obtained for a sample of starburst galaxies (Calzetti et al. 1994). We consider the upper limits as positive detections, and we verify that the model-predicted fluxes are consistent with the data, i.e. equal to or below the upper limits.

**Table 1.** Lower limits to the visual extinction towards GRB 100614A and GRB 100615A.

GRB	$t - T$ min	$\beta_X$	$A_{V,MW}$ mag	$A_{V,SMC}$ mag	$A_{V,SB}$ mag
14A	258	1.20	8	8	6
<b>14A</b>	<b>258</b>	<b>1.50</b>	<b>13</b>	<b>13</b>	<b>8</b>
14A	258	1.80	18	18	11
14A	570	1.20	25	31	6
<b>14A</b>	<b>570</b>	<b>1.50</b>	<b>47</b>	<b>58</b>	<b>11</b>
14A	570	1.80	69	85	17
15A	24	1.20	39	47	10
<b>15A</b>	<b>24</b>	<b>1.35</b>	<b>49</b>	<b>60</b>	<b>13</b>
15A	24	1.50	59	73	16
15A	330	1.20	47	58	12
<b>15A</b>	<b>330</b>	<b>1.35</b>	<b>58</b>	<b>72</b>	<b>15</b>
15A	330	1.50	69	86	18
15A	13200	1.20	12	15	3
<b>15A</b>	<b>13200</b>	<b>1.35</b>	<b>22</b>	<b>27</b>	<b>6</b>
15A	13200	1.50	33	40	9

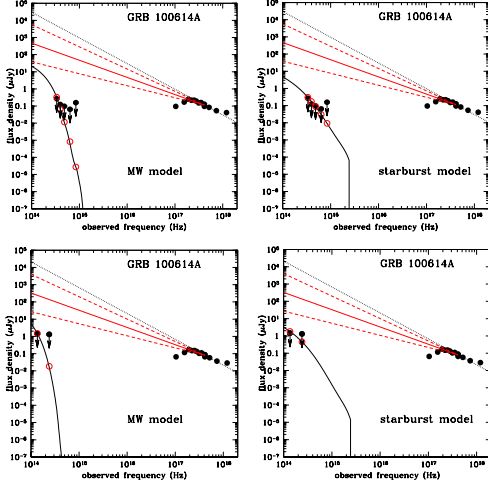


**Fig. 2.** GRB 100614A SEDs at two different epochs: GTC *ugriz* upper limits taken 4.3 hours after the trigger (upper panels) and the NIR J and K band taken 9.5 hours after the trigger (lower panels), with  $\beta_{OX}$  fixed at  $\beta_X - 0.5$  (solid red line) and the optical suppression modelled with the MW or starburst extinction curves. Black dotted line represents the best-fit value for the X-ray spectral slope ( $\beta_X = 1.50$ ). Dashed red lines enclose the 90% uncertainty in  $\beta_{OX}$ .

### 3. Results

We find that GRB fluxes computed from both optical and NIR data are well below the most conservative extrapolation from X-rays and require strong absorption using the data taken within 1 day after the trigger. For GRB 100615A, very late-time data are available (9.2 days after the trigger), for which the NIR flux is still below the X-ray extrapolation.

The GRB 100614A SED with the reddest flux upper limit (i.e. 570 minutes after the trigger) requires a rest-frame V-band dust extinction of  $A_V \geq 47$ , 58, and 11 mag, assuming a MW, SMC, or a starburst attenuation curve, respectively, and using the best-fit value for  $\beta_X$  (Fig. 2). Even fixing the optical to X-ray energy spectral index to its lowest allowed value (within its 90% confidence range), that is, in the most conservative case, results still provide very high  $A_V$  lower limits (Table 1). Less stringent constraints on  $A_V$  are obtained using the

GTC *ugriz* flux upper limits obtained 258 minutes after the trigger. We obtain  $A_V \geq 13$  mag with either the MW and SMC extinction curve and  $A_V \geq 8$  mag with the starburst case.

For GRB 100615A, we obtain even tighter lower limits. The SED extracted 24 minutes after the burst requires  $A_V \geq 64$ , 79, or 16 mag assuming either a MW or SMC extinction curve, or a starburst attenuation curve, respectively. These lower limits are still very high for the SED extracted 5.5 hours post burst:  $A_V \geq 58$ , 72, and 15 mag for the three extinction recipes. Less critical but still high values, are obtained even 9.2 days from the burst:  $A_V \geq 22$ , 27, and 6 mag (Fig.3). The latter lower limits are lower than the ones obtained at earlier epochs (but still extreme), possibly due to a selection effect, since at later times the X-ray flux decreases, but the optical/NIR upper limits can not become fainter consistently, owing to the instrument detection limits.

Table 1 reports all the  $A_V$  lower limits evaluated from the GRB 100614A and GRB 100615A data at the given mean observation epochs. These lower limits are computed for the reported ranges of the X-ray spectral index ( $\beta_X = \Gamma - 1$ , estimated in Sect. 3) that corresponds to the minimum, maximum, and mean value of the estimated 90% confidence range. Bold face characters indicate the results obtained with the most probable X-ray spectral index. Upper limits to the optical-to-X-ray spectral indices  $\beta_{OX}$  are also shown.

### 4. Discussion

We have analyzed two *Swift* ‘dark’ GRBs, namely, GRB 100614A, and GRB 100615A. These GRBs are dark according to every definition proposed until now. They are not detected in the optical/NIR down to very faint limits, despite follow-up campaigns at ground-based facilities began minutes to hours from the BAT triggers (see Table 1). In addition, their optical-to-X-ray spectral indices satisfy  $\beta_{OX} < \beta_X - 0.5$  (van der Horst et al. 2009 criterion). The identification of these two GRBs as dark bursts is the consequence of their intense X-ray flux coupled to the optical/NIR missing detections.

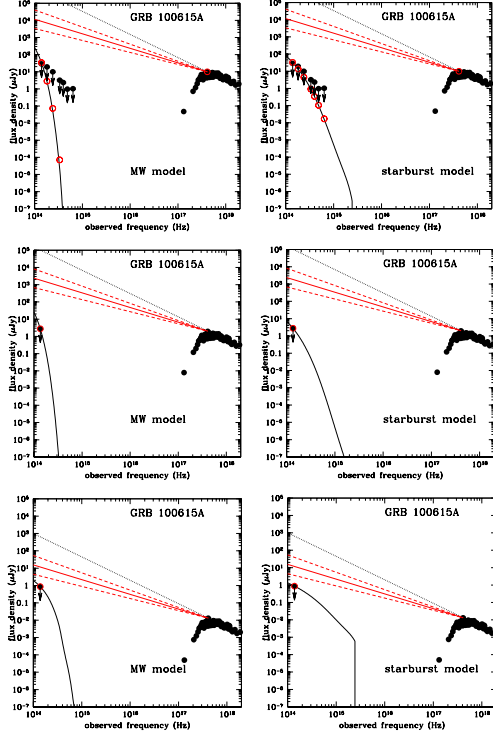


**Fig. 3.** GRB 100615A SEDs at three different epochs: GROND *grizJHK* upper limits taken 24 minutes after the trigger (upper panels) and Gemini-North K and Ks upper limits taken 5.5 hours and 9.2 days after the trigger, respectively (middle and lower panels), with  $\beta_{OX}$  fixed at  $\beta_X - 0.5$  and the optical suppression modelled with the MW or starburst extinction curves. Black dotted line represents the best-fit value for the X-ray spectral slope ( $\beta_X = 1.35$ ). Dashed red lines enclose the 90% uncertainty in  $\beta_{OX}$ .

The outcome of our analysis is surprising. To explain the deepest NIR upper limits (i.e. the less affected by dust) in terms of a flux suppression described by either a MW or SMC dust extinction laws,  $A_V > 47$  ( $A_V > 58$ ) mag is needed for GRB 100614A (GRB 100615A) before one day and  $A_V > 22$  at 9 days after the trigger for GRB 100615A. Such extreme  $A_V$  values have never been observed before and require an explanation.

While a SMC-like extinction curve can adequately fit a large fraction of the dust extinction from GRB host ISM, our present picture

of GRB host galaxies makes an extremely obscured environment of this kind a very unlikely possibility. Indeed, GRBs, even reddened ones, are hosted by blue or normal galaxies, which are commonly detected in ordinary galaxy surveys. This favours a scenario of a host morphology where the line of sight to the GRB is dusty, i.e., dust obscures only localized regions (see e.g., Perley et al. 2009 and references therein). An in situ obscuration appears to be insufficient to be responsible for the extreme extinction levels we measure.

All these considerations hold if the optical radiation and X-rays are part of the same synchrotron spectrum. They could originate from different emission processes or even be produced in different, independent emission regions. This is possible in particular during the so-called “shallow phase”, where X-ray emission may be dominated by an emission component that differs from the one from which the optical flux originates (e.g. Zhang 2007). Since the two SEDs of GRB 100614A, the first one of GRB 100615A, and (marginally) the second one of GRB 100615A are all extracted during the shallow phases of these GRBs, a different origin of the optical and X-ray emission in these epochs could at least in part explain the optical darkness of our GRBs. However, we note that for GRB 100615A we have extracted a SED at a very late time, about nine days after the end of the plateau phase, and we have still obtained very high  $A_V$  lower limits ( $A_V > 20$ ) assuming either a MW or a SMC extinction curve. These values are less extreme than that obtained using the other SEDs, but still very high, suggesting another or at least a concurring mechanism to account for the GRB darkness.

This complementary explanation could be that local extinction recipes, such as MW or SMC ones are inadequate for reproducing the optical suppression in the host galaxies of these two GRBs. For example, modelling the dust absorption using greyer extinction laws, such as the attenuation curve obtained from the observations of starburst galaxies proposed by Calzetti (1994), brings GRB 100614A and GRB 100615A to require  $A_V$  lower limits that are less extreme, despite still being very high.

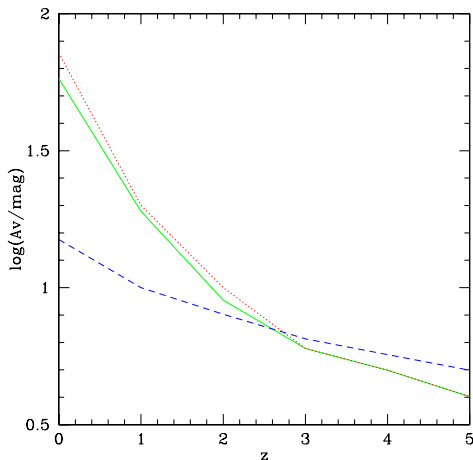


**Fig. 4.** The visual extinction  $A_V$  as a function of redshift for the second epoch SED of GRB 100615A. Green solid, red dotted, and blue dashed lines are for the Milky Way, Small Magellanic Cloud, and starburst recipes, respectively.

A mixture of moderate-to-high redshift and extinction can reduce the dust level necessary to explain the SEDs. In Fig. 4, we plot as an example the  $A_V$  values as a function of  $z$  obtained for the second epoch of GRB 100615A observations. Although the visual extinction is considerably lower than for the  $z = 0$  case,  $A_V \sim 10$  at  $z = 2$  and  $A_V \sim 4 - 5$  at  $z = 5$  is still required, regardless of the adopted extinction recipe. Thus, an intrinsic origin and/or dust extinction, coupled to a moderately high redshift could explain the darkness of our GRBs.

A more exotic but intriguing possibility would be that these GRBs are extremely high redshift events. Assuming that the lack of any detection in the reddest NIR band (K-band) is due to Ly $\alpha$  absorption from the intergalactic hydrogen neutral fraction, we can set a redshift lower limit of  $z > 17$ . The first population of very massive stars (PopIII,  $10^2 M_\odot < M < 10^3 M_\odot$ ) is expected to form at  $z \sim 20$ . Their death is supposed to leave behind black holes of several tens of solar masses, which could be the early progenitors of active galactic nuclei.

These fast-spinning black holes have a rotational energy of  $\sim 10^{55}$  erg or more that can power a GRB explosion. The isotropic energies of GRB 100614A and GRB 100615A assuming  $z = 18$  are  $1.3 \times 10^{54}$  erg and  $7.2 \times 10^{53}$  erg, respectively (using the BAT fluences). However, the reported isotropic energies must be considered as lower limits both because of the conservative choice of the  $z$  used and because the BAT detector does not constrain the position of the peak emission preventing a bolometric estimate of the emitted energy. The lack of detection of any host galaxy candidate for these GRBs represents additional support of this scenario. On the other hand, against the high redshift interpretation there is that the expected GRB rate at  $z > 17$  is extremely low, between 0.5 and 1 GRB every 10 yr (Bromm & Loeb 2006).

A possible way to differentiate between extremely high-redshift, exotic extinction recipes and emission from distinct components for sources such as these, would be to search for the afterglow in the mid- or far-IR bands. A non-detection also in these bands could hardly be explained using any extinction law and would definitely rule out a high redshift origin. A multiband detection compatible with the X-ray flux at late times (e.g.  $> 10^5$  s after the trigger, i.e. after the end of the “shallow phase”) would instead favour the fireball model. In this case, given the lack of NIR detections, the origin of the darkness would be in exotic extinction or high redshift, depending on the spectral shape in the mid- and far-IR bands.

## References

- Bromm G. & Loeb A. 2006, ApJ, 642, 382
- Calzetti D. et al. 1994, ApJ, 429, 582
- D’Elia, V. & Stratta, G. 2011, A&A, 532, 48
- Groot P.J. et al. 1998, ApJ, 493, L27
- Perley D.A. et al. 2009, AJ, 138, 1690
- van der Horst, A.J. et al. 2009, ApJ 699, 1087
- van Paradijs, J. et al. 1997, Nat, 383, 686
- Zhang B. 2007, ChJAA, 7, 1